

Controlling non-Abelian statistics of Majorana fermions in semiconductor nanowires

Jay D. Sau,¹ David J. Clarke,² and Sumanta Tewari³

¹*Condensed Matter Theory Center and Joint Quantum Institute, Department of Physics,
University of Maryland, College Park, Maryland 20742-4111, USA*

²*Department of Physics and Astronomy, University of California, Riverside, CA 92521, USA*

³*Department of Physics and Astronomy, Clemson University, Clemson, SC 29634*

Under appropriate external conditions a semiconductor nanowire in proximity to an s -wave superconductor can be in a topological superconducting (TS) phase. This phase supports localized zero-energy Majorana fermions at the ends of the wire. However, the non-Abelian exchange statistics of Majorana fermions is difficult to verify because of the one-dimensional topology of such wires. In this paper we propose a scheme to transport Majorana fermions between the ends of different wires using tunneling, which is shown to be controllable by gate voltages. Such tunneling-generated hops of Majorana fermions can be used to exchange the Majorana fermions. The exchange process thus obtained is described by a non-Abelian braid operator that is uniquely determined by the well-controlled microscopic tunneling parameters.

PACS numbers: 03.67.Lx, 03.65.Vf, 03.67.Pp, 05.30.Pr

I. INTRODUCTION

Majorana fermions (MFs) have been the subject of intense recent study in part due to their potential application in topological quantum computation (TQC).^{1–7} Unlike ordinary fermionic or bosonic operators for which the particle creation operators are the hermitian conjugate of the annihilation operators, MF operators, γ , are self-adjoint ($\gamma^\dagger = \gamma$). In this sense, MFs are their own anti-particle and the realization of such excitations would be the first example of such particles which had been proposed more than seventy-five years ago.⁸ MFs are of interest for TQC because despite having no internal degrees of freedom individually, a pair of MFs, say γ_1 and γ_2 , have two distinct possible states (fusion channels). These states, which may be thought of as the two possible occupation states of the complex fermionic operator $c^\dagger = \frac{\gamma_1 + i\gamma_2}{2}$, are energetically degenerate to a degree exponential in the separation of the Majorana fermions, and correspond to the eigenstates of the combined operator $\gamma_1\gamma_2$, with eigenvalues ± 1 . Such a topological protected degeneracy has yet to be seen in nature, and the observation of such would be a major breakthrough in physics. The central idea of TQC is to use the topologically degenerate states of a pair of MFs as a 2-level topological qubit which would in principle be protected from decoherence. The manipulation of the information contained in the topological qubits requires the use of topological braid operations which consists of moving the MFs around one another.

In the past few years, topological superconductors have become promising candidates for realizing MFs.^{9–16} Recently, it has been proposed that a semiconductor thin film with Rashba-type spin-orbit (SO) coupling together with proximity-induced superconductivity and Zeeman splitting would be a suitable platform for realizing a Majorana-fermion-carrying topological superconducting (TS) state.^{17–20} The s -wave superconducting pairing potential can be induced in the semiconductor system by placing it in proximity to a conventional superconductor such as aluminum. The Zeeman splitting can similarly be induced, in principle, by proximity to a magnetic-insulator.²⁰ The one-dimensional ver-

sion of this system, i.e. a semiconducting nanowire with proximity-induced s -wave superconductivity, has also been shown to host MF as zero-energy modes at the ends of the wire under appropriate conditions.^{21,22} The one-dimensional nanowire geometry has the specific advantage that the Zeeman splitting V_Z in the nanowire is not required to be proximity-induced from a magnetic insulator, but instead can be introduced by a magnetic field parallel to the nanowire.²² Such a parallel magnetic field would not introduce unwanted orbital effects such as vortices if a thin-film superconductor is used to generate the superconducting proximity-effect. The proposed semiconducting structures exist in a TS phase and supports MFs at its ends when the s -wave superconducting pair potential Δ , Zeeman splitting V_Z , and the chemical potential μ satisfy the condition $V_Z^2 > \Delta^2 + \mu^2$.^{17,20,22} Thus the chemical potential μ , which can be controlled by an external gate potential, can be used to tune a nanowire from the TS phase to a non-topological (NTS) phase. In fact, the s -wave proximity effect on a InAs quantum wire, which also has a sizable SO coupling, may have already been demonstrated in experiments.²³ These semiconductor based proposals for realizing a TQC platform can take advantage of the considerably advanced semiconductor fabrication technology. Therefore, it seems that a Majorana-carrying TS state in a semiconductor quantum wire may be within experimental reach.

Until recently, motivated by experiments, most discussions of observing non-Abelian statistics using MFs has been restricted to 2D systems. In 2D non-Abelian systems, the quantum information associated with MFs can be manipulated in a topologically protected manner by exchanging the Majorana bound states (e.g., by adiabatically moving vortices in $p+ip$ superconductors).^{24,25} The protection of the topological degeneracy associated with MFs requires the MFs to remain spatially separated at all steps of the exchange. Therefore, at first glance, it appears that it is impossible to exchange the MFs at the ends of a 1D wire, since any such attempt would necessarily lead to the spatial overlap of MFs at some stage of the overlap process. A solution to this problem has been provided by Alicea *et al.*²⁶, who have shown that connecting up a system of nanowires into a network allows one to

exchange MFs. In their proposal, the two MFs, γ_1 and γ_2 , at the ends of a wire can be exchanged by introducing an additional nanowire B . The additional nanowire, B , allows one to temporarily move one of the MFs, say γ_1 , away from the original nanowire, A , so that the other MF γ_2 can be moved across the wire A without colliding with γ_2 . The MF γ_1 can then be returned from the wire B back to its original wire A . While this scheme solves the basic problem of non-Abelian statistics in 1D, it requires the transport of a MF across a tri-junction between two topological nanowires A and B , which is potentially a more complex topological object than the simple topological nanowire. The continuous transport of MFs through such a tri-junction is potentially dependent on details of the junction that may be difficult to control.²⁷ Moreover, from a theoretical point of view, the explicit determination of the non-Abelian statistics in this geometry in terms of the microscopics of the junction is somewhat complicated.

In this paper we propose an alternative scheme to transport MFs at the ends of one dimensional semiconductor nanowires where the ends of the nanowires remain fixed, but the tunneling amplitudes between the end MFs are varied. Bringing the end MFs closer together allows one to create a non-vanishing Hamiltonian of the MFs which can generate effecting MF hopping from one end site to another. Using this picture of a dynamically changing tunneling Hamiltonian, we will be able to derive a simple explicit expression for the non-Abelian statistics transformation of the MFs in terms of tunneling matrix elements.

II. OUTLINE AND SUMMARY OF RESULTS

As mentioned in the previous paragraph, MFs are strictly zero-energy modes with an associated topological degeneracy only in the limit when they are separated by a distance that is large compared to the decay length of the MFs. The two states of the MFs γ_1 and γ_2 can be described in terms of the 2 possible occupation states of the Dirac fermion $c^\dagger = \gamma_1 + i\gamma_2$. These 2 states correspond to the eigenvalues 0 and 1 of the number operator $n = c^\dagger c = \frac{1+i\gamma_1\gamma_2}{2}$. In general, the Hamiltonian for a pair of MFs with a non-negligible splitting produces a splitting between the 2 energy states and can be written as

$$H_{\text{tunneling}} = i\zeta_{12}(x)\gamma_1\gamma_2 \quad (1)$$

where $\zeta_{12}(x)$ is the tunneling matrix element for the MFs which depends on the separation x between the MFs γ_1 and γ_2 .²⁵ The energy splitting between the $n = 0$ and $n = 1$ states is given by $|\zeta_{1,2}(x)|$. Therefore, the topological degeneracy of MFs emerges only in the limit $x \gg \xi$ when the MF overlap matrix-element $\zeta_{12}(x)$ vanishes because of the localization of the MF wave-functions. Here ξ is the localization length of the MFs. The tunneling of MFs at the ends of different wires, whose ends are placed close together, is entirely analogous to the tunneling of electrons between two quantum dots which can be controlled by raising and lowering the barrier between the dots. Similarly, tunneling amplitudes between MFs on different semiconductor nanowires can be controlled simply by

adding a gate controllable tunnel barrier between the MFs.³⁰ Gate voltages can also induce tunneling between MFs at the ends of the same TS segment by tuning the nanowire close to a TS-NTS phase transition.²⁰ Bringing the nanowire close to the TS-NTS transition, decreases the gap of the system which in turn increases the localization length ξ of MFs in the wire and allows the tunneling between the initially localized MFs at the ends of TS segments. The quantitative details of how the tunneling is controlled in topological nanowires is discussed in the appendix.

Tunneling of ordinary fermions such as electrons can be used to move electrons from one quantum dot to another in a system of quantum dots. In this paper, we will show that the same principle applies to MFs, and repeated use of the tunneling Hamiltonian in Eq. 1 can be used to exchange MFs γ_1 and γ_2 in a system of TS nanowires that hosts such MFs at its ends. The unitary time-evolution operator U associated with the exchange maps $\gamma_1 \rightarrow U\gamma_1U^\dagger = \lambda\gamma_2$ and $\gamma_2 \rightarrow U\gamma_2U^\dagger = -\lambda\gamma_1$ where λ can be directly computed from the tunneling matrix elements $\zeta_{i,j}$ involved in moving the MF γ_1 to the starting position of the MF γ_2 . In the low-energy subspace of MFs, the time-evolution operation U , that describes the exchange process has the usual form of a braid matrix²⁴

$$U = e^{\frac{\pi}{4}\lambda\gamma_1\gamma_2}. \quad (2)$$

While there are only two possible answers $\lambda = \pm 1$ for the braid-matrix, it is critical to be able to determine the factor λ for a given braid since this is what distinguishes 'clock-wise' from 'counter-clock-wise' exchanges. For the specific geometry discussed in the appendix with wires placed in a superconducting film together with an in-plane magnetic field at 45 degrees to the wires, the sign of the braid matrix, λ , is determined by the sign of the Rashba spin-orbit coupling constant α .

The braiding scheme we will discuss is potentially related to measurement-only schemes for braiding of topological quasiparticles.^{28,29} However, it is not clear how the anyon model postulates assumed in the measurement-only theory apply to the superconducting nanowire systems described by mean-field BCS theory. For example, the identification of the tunneling matrix element between MFs in Eq. 1 with the topological charge measurement in Ref. 29 becomes subtle in cases where the sign of the tunneling $\zeta_{12}(x)$ oscillates in sign with the separation x . On the other hand the approach in this paper is based only on the MF tunneling Hamiltonian Eq. 1, which can be derived microscopically from BCS Hamiltonians.³¹ The tunneling matrix elements $\zeta_{ij}(x)$ themselves depend on the details of the nanowire system such as the spin-orbit coupling, the orientation of the wire and the Zeeman splitting. Therefore, we first consider exchange of MFs around a specific triangular loop geometry in terms of the tunnel matrix elements between the various MFs and then in the appendix, we show how the microscopic tunneling parameters may be calculated in one specific geometry. As a result of our calculation, we find that for general values of the tunneling, the parameter λ in the braid matrix U has the simple form $\lambda = \text{sgn}(\zeta_{12})\chi$ where χ is the junction chirality of the

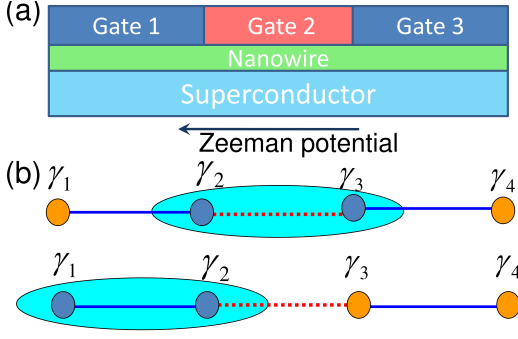


FIG. 1: (Color online)(a) Combination of SC, Zeeman and gate potentials leads to nanowire segments in TS and NTS phases. The gates 1 and 3 are adjusted such that the nanowire is in TS phase, while 2 is adjusted so that the wire is in NTS phase corresponding to the schematic in panel (b). (b) Nanowire segments in TS phase are shown as blue (solid) lines and NTS segments are shown as red (dotted) lines. Orange (light) and blue (dark) circles indicate unpaired and paired MFs at TS-NTS interfaces, respectively. MFs are paired by tunneling across the TS or NTS segments denoted by light blue oval. Decreasing the tunneling amplitude between γ_2 and γ_3 and simultaneously increasing the tunneling amplitude between γ_1 and γ_2 can effectively transfer MF $\gamma_1 \rightarrow \gamma_3$.

triangular loop that we will define as the product of tunnelings around the loop. Finally, we would like to note, that while the motivation of exchanging MFs is to be able to manipulate the information contained in topological qubits constructed from MFs in an effort to perform TQC, it is well-known that braiding by itself is insufficient for TQC.⁶ However, MF exchanges are still crucial as one of the most direct tests of non-Abelian statistics and probably also for any future TQC schemes using MFs.

III. MF TRANSPORT

To understand how MF transport in a system of nanowires can be induced by tunneling, consider the simple system of nanowires shown in Fig. 1(a) consisting of three semiconducting nanowire segments. Two of these segments (shown by solid blue lines in the schematic in Fig. 1(b)) are in the TS phase, while the wire shown with the red dashed line is in the NTS phase and serves as the tunnel barrier connecting MFs. Each end of the wires in the TS phase supports a MF (shown as discs). In the initial state (shown in the upper panel of Fig. 1(b)), the gate voltage of the NTS segment is chosen to allow a finite tunneling amplitude (shown by light blue oval) across it. This pairs up the MFs γ_2 and γ_3 into finite energy states with a gap. Thus the operators $\gamma_{2,3}$ become gapped MFs (shown as dark blue discs) and cannot be used to store quantum information as can be done with the true zero-energy MFs (shown as light orange discs). The transfer of the MF from position 1 to 3 is achieved by adiabatically deactivating the tunneling in the NTS segment 2 – 3 and activating the tunneling in the TS segment 1 – 2.

The process of transferring the MF from position 1 to 3

shown in Fig. 1(b) is described by the time-dependent tunneling Hamiltonian that is derived by extending the tunneling Hamiltonian in Eq. 1 and can be written as

$$H = [\zeta_{12}\alpha(t)\gamma_1\gamma_2 + \zeta_{23}(1 - \alpha(t))\gamma_2\gamma_3] \quad (3)$$

where ζ_{12} and ζ_{23} are the activated tunneling amplitudes across the segments 1 – 2 and 2 – 3 respectively. Over the transfer process $\alpha(t)$ varies adiabatically from $\alpha(0) = 0$ to $\alpha(t_1) = 1$. It is convenient to understand the braiding procedure for MF operators in the Heisenberg representation $\gamma_j(t) = U^\dagger(t)\gamma_j U(t)$ where the U is the unitary time-evolution operator $U(t) = Te^{-i\int_0^t H(\tau)d\tau}$ (which is a time-ordered exponential). The operators $\gamma_j(t)$ can be computed from the Heisenberg equation of motion $\dot{\gamma}_j(t) = i[H^{(H)}(t), \gamma_j(t)]$. The Hamiltonian (Eq. 3) describing the evolution of $\gamma_j(t)$ can be written compactly in terms of an effective B-field ($B_j(t)$) as

$$H^{(H)}(t) = \sum_{a,b,c=1,2,3} \epsilon_{abc} B_a(t) \gamma_b(t) \gamma_c(t) \quad (4)$$

where ϵ_{abc} is the anti-symmetric Levi-Civita tensor. The time-dependent B-field given by

$$\mathbf{B}(t) = (1 - \alpha(t))\zeta_{23}(1, 0, 0) + \alpha(t)\zeta_{1,2}(0, 0, 1). \quad (5)$$

The Heisenberg equation of motion for $\gamma_a(t)$ takes the form

$$\dot{\gamma}_a = 2\epsilon_{abc} B_b(t) \gamma_c(t). \quad (6)$$

This equation of motion is identical to that of the spin operators $\sigma_a(t)$ of a spin-1/2 particle in a time-dependent magnetic field $\mathbf{B}(t)$ (with a Hamiltonian $H^{(H)}(t) = -\mathbf{B}(t) \cdot \boldsymbol{\sigma}(t)$). Furthermore, the initial condition on the operator $\gamma(t) = \gamma_1$ corresponds to the spin-operator $\sigma(t) = \sigma_1(0)$ in an initial effective magnetic field $\mathbf{B}(0) = \zeta_{23}(1, 0, 0)$ that is aligned or anti-aligned with σ_1 . Thus, after a time-evolution under an adiabatically varying magnetic field, the spin (and correspondingly the MF) remains aligned or anti-aligned with the final magnetic field $\mathbf{B}(t_1) = \zeta_{12}(0, 0, 1)$ at time $t = t_1$. This leads to the expression

$$\gamma_3(t_1) = \text{sgn}(\zeta_{12}\zeta_{23})\gamma_1(0). \quad (7)$$

Thus the transfer of the tunneling amplitude from the segment 2 – 3 to the segment 1 – 2, leads to transport of the MF from position 1 to position 3. The hopping of MFs between sites described by Eq. 7 is identical to the motion of regular fermionic operators under that action of tunneling. We will represent this process by the MF trajectory

$$1 \xrightarrow{2} 3. \quad (8)$$

The result in Eq. 7 is consistent with a somewhat different approach suggested by Kitaev.³²

IV. MFS AS DEFECTS IN DIMER LATTICES

In the previous section, we saw that to transport a single MF from one position to another it was necessary to make use

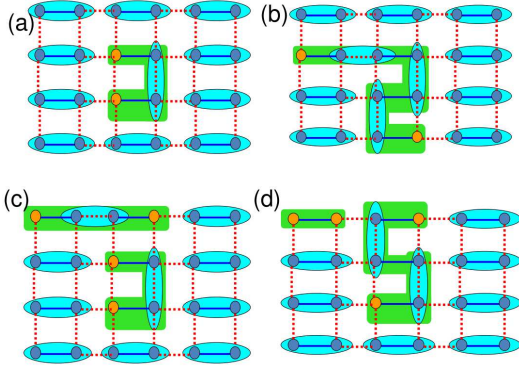


FIG. 2: (Color online)(a) Configuration of TS nanowires in a square dimer lattice with 2 isolated MFs. MFs are effectively bound to defects (unpaired sites) on the dimer lattice. Tunneling between different TS segments fuses TS wires into isolated effective 'topological wires' shown in green (gray) blocks with MF end modes. (b) MF transfer processes analogous to Fig. 1 can extend effective TS wires and move MFs in dimer lattice in a way analogous to Alicea et al.²⁶. (c) and (d): Similar transfer processes can be used to switch the MF end modes between different effective 'topological wires'. All operations of the MF square lattice either exchange, contract or switch ends of different 'topological wires'.

of another pair of MFs which were coupled by a weak tunneling so that they were not strictly zero-energy MFs. The single MF being exchanged had to be a true zero-energy MF with no tunneling, while the pair of MFs with tunneling between them may be thought of as a gapped MF dimer. Exchanges of true zero-energy MFs requires a generalization of this picture to include several isolated MFs which are not coupled to any other MF by tunneling. As is clear from Fig. 1(b), such a process also requires a supply of gapped pairs of MFs (i.e. MF dimers). In this paper, we will consider a system of nanowires with end MFs most of which are paired up by tunneling into MF dimers as shown in Fig. 2(a). If all MF sites are completely paired up, then the system has no true zero-energy MFs and no topological degeneracy or non-Abelian statistics. Therefore we consider a system, where in addition to the MF dimers, there are a few isolated MFs that are unpaired by tunneling. If one considers a regular lattice of nanowires so that the end MFs live on the vertices of a square lattice (Fig. 2), a system of dimerized MFs forms a dimer covering of the lattice, while isolated MFs are associated with defects (unpaired sites) in the MF dimer lattice. As seen by comparing Fig. 2(a) and (b), the transport of MFs on the dimer-lattice is obtained by changing the dimerization pattern on the dimer lattice analogous to Fig. 1(b).

The MFs on the dimer lattice can also be thought of as the end points of topological wires. To see this we define effective 'topological wires', shown by green (gray) boxes in Fig. 2, by considering TS wire segments coupled by tunneling as a single topological wire. This identification, relates our proposal in a direct way to the proposal of Alicea et al.²⁶ However, the details of the physical implementation remain different and the dimer implementation presented in this paper will allow us

to directly use Eq. 7, to determine the form of the braid-matrix in Eq. 2. The continuous processes required by Alicea et al. for exchanging MFs were extending and contracting topological wire segments together with an operation that we will refer to as exchanging the ends of different topological wires. This process required bringing together a pair of topological wires in a tri-junction and effectively takes a pair of topological wires with end points $\gamma_{1,2}$ and $\gamma_{3,4}$ and creates a new pair of wires with end points $\gamma_{1,3}$ and $\gamma_{2,4}$. All these processes can be accomplished in MF dimer lattice by repeated application of the process shown in Fig. 1 associated with Eq. 7. The analogue of the extension and contraction process in a dimer lattice is shown in Fig. 2(a) and (b), while the end switching process is shown in Fig. 2(c) and (d).

V. NON-ABELIAN STATISTICS OF MFS IN NANOWIRES

In this section, we show explicitly, that exchange of MFs in any dimer lattice can always be described by an equation of the form of Eq. 2. Unpaired MFs can be exchanged via discrete tunneling operations of the form shown in Fig. 1(b). Since the physical positions of the MFs are exchanged by the correct sequence of MF transfers, the resulting transformation of the MFs at the end of the transformation $t = t_{final}$ has the general form

$$\begin{aligned}\gamma_1(t_{final}) &= \lambda \gamma_2(0) \\ \gamma_2(t_{final}) &= \tilde{\lambda} \gamma_1(0).\end{aligned}\quad (9)$$

However, consistency with non-Abelian statistics also require us to prove that $\lambda\tilde{\lambda} = -1$. If $\lambda\tilde{\lambda} = -1$, the exchange transformation can be represented by the operator U of the form Eq. 2.

To show $\lambda\tilde{\lambda} = -1$, let us label the unpaired MFs, which are to be exchanged as 1 and 2 and take all other MFs as paired, $(2n-1, 2n)$ for $n = 2, \dots, N$. The positions of the MFs following each step (labelled by the index p) of the exchange process, which permutes the positions of the MFs, can be represented by the function $\pi_p(j)$, where $j = 1, \dots, 2N$ is the MF index. After each step p , the MF coordinates are updated from π_{p-1} to π_p according to the relation

$$\pi_p(j) = \pi_{p-1}(C_p(j)) \quad (10)$$

where C_p is a cyclic (clockwise or anticlockwise) permutation of the MFs $a_p, 2n_p - 1$ and $2n_p$ corresponding to Eq. 7. Here we choose a_p to be one of the unpaired MFs, 1 or 2, and $n_p > 1$ such that MF dimer $(2n_p - 1, 2n_p)$ is paired. The equation of motion for the unpaired Majorana operators corresponding to Eq. 7 is

$$\gamma_{\pi_{p+1}(a_p)}(t_{p+1}) = \lambda_p \gamma_{\pi_p(a_p)}(t_p). \quad (11)$$

where

$$\lambda_p = \text{sgn}(\zeta_{\pi_{p+1}(2n_p-1)\pi_{p+1}(2n_p)} \zeta_{\pi_p(2n_p-1)\pi_p(2n_p)}). \quad (12)$$

The total sign $\lambda\tilde{\lambda}$ picked up by the unpaired MFs is the product $\lambda\tilde{\lambda} = \prod_p \lambda_p$. To calculate this product we define a sequence $Q_p = \text{sgn}(\prod_{n>1} \zeta_{\pi_p(2n-1), \pi_p(2n)})$. From Eq. 12 it

follows that $Q_{p+1} = \lambda_p Q_p$ so that

$$Q_{final} = \lambda \tilde{\lambda} Q_{p=0}. \quad (13)$$

Note that since each cyclic permutation C_p contains even number of exchanges (i.e. is an even permutation), the permutations π_p at each step (including the final permutation π_{final}), which is a product of C_p s, is also an even permutation.

Since the Hamiltonian is required to return to its initial configuration, the MFs at positions $(2n-1, 2n)$ must be paired by tunneling for $n > 1$. This requires that π_{final} is composed of a pair exchange of the positions of MF dimers $(2n-1, 2n) \leftrightarrow (2n'-1, 2n')$ together with possible internal flips $(2n-1 \leftrightarrow 2n)$ of the dimers. Since, π_{final} is an even permutation, and dimer exchanges are even permutations, the number of internally flipped dimers $(2n-1 \leftrightarrow 2n)$ in π_{final} is even. Moreover, the unpaired pair of MFs $(1, 2)$ is flipped in π_{final} . Thus an odd number of the paired MF dimers $(2n-1 \leftrightarrow 2n)$, must be flipped for $n > 1$. Each such dimer flip changes the sign of Q_{final} , since $\zeta_{2n-1, 2n} = -\zeta_{2n, 2n-1}$ for $n > 1$. This leads to the relation $Q_{final} = -Q_{p=0} = \lambda \tilde{\lambda} Q_{p=0}$, proving the consistency condition for non-Abelian statistics i.e. $\lambda \tilde{\lambda} = -1$.

VI. EXCHANGE AROUND A TRIANGULAR LOOP

A specific realization of the non-Abelian statistics in nanowire systems is provided by a triangular loop geometry shown in Figs. 3 and 4. The triangular loop consists of one end (A_2, B_2 and C_2) of each of three TS segments (A, B and C) connected by NTS segments to form a triangle. The other ends are labeled A_1, B_1 and C_1 . The MFs to be exchanged, referred as 1 and 2, are assumed to be localized at 2 of these 6 ends of TS segments. Each of the steps for the MF exchange (shown in Figs. 3 and 4) consists of moving exactly one MF from one position to the other (shown by dotted arrows) by adiabatically turning off the tunneling in some wire segment and increasing it in an adjoining segment as discussed before.

The procedure to exchange the MFs 1 and 2 at the ends of different TS segment through the tri-junction takes place in four steps shown in Fig. 3. The signs associated with the exchange λ and $\tilde{\lambda}$ can be determined by following the trajectories of the MFs 1 and 2 and applying Eqs. 7 and 9. From Fig. 3, it is clear that the sequence of positions followed by the MFs 1 and 2 are

$$\begin{aligned} \text{MF 1: } A_2 &\xrightarrow{(3)} C_2 \xrightarrow{(2)} B_2 \\ \text{MF 2: } B_2 &\xrightarrow{(2)} C_1 \xrightarrow{(4) \equiv (1)} A_2 \end{aligned} \quad (14)$$

respectively. Here we show only the MF that is moved in each step, which is numbered in Fig. 4 as ($j = 1, \dots, 4$) (marked below the arrows in Eq.14). The MF motion is shown using the notation defined in Eq. 8 so that the sign can be calculated using Eq. 7. Applying Eq. 7, the parameters λ and $\tilde{\lambda}$ simplify

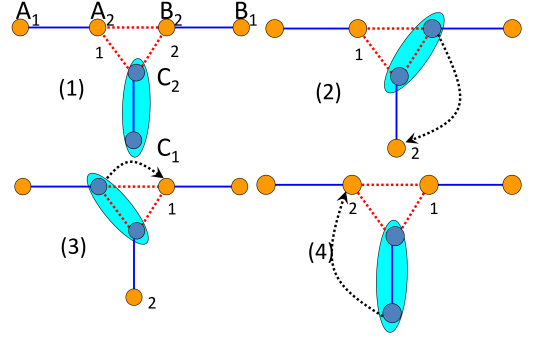


FIG. 3: (Color online) MFs 1 and 2 at the ends of different TS segments are exchanged. This is achieved by switching tunnelings on and off on TS and NTS segments in 4 steps going from a state shown in one panel to the next panel. Dotted arrow shows motion of MF from the previous panel. The labelling for the sites A_1, A_2, B_1, B_2, C_1 and C_2 is shown in panel (1).

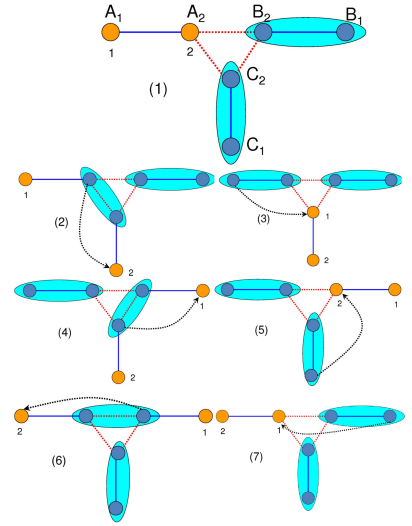


FIG. 4: (Color online) MFs 1 and 2 at the ends of the TS segment on the left leg are exchanged in seven steps similar to Fig. 3. Step (7) transfers state shown in panel (6) back to panel (1) with the effect that the Majoranas 1 and 2 are interchanged.

to

$$\lambda = -\tilde{\lambda} = \text{sgn}(\zeta_{A_2 B_2}) \chi \quad (15)$$

where $\chi = \text{sgn}(\zeta_{A_2 B_2} \zeta_{B_2 C_2} \zeta_{C_2 A_2})$ is defined to be the chirality of the tri-junction.²⁷

Similarly MFs at the ends of the same TS segment can be exchanged using six steps shown in Fig. 4. From Fig. 4, it is clear that the sequence of positions followed by the MFs 1 and 2 are

$$\begin{aligned} \text{MF 1: } A_1 &\xrightarrow{(3)} C_2 \xrightarrow{(4)} B_2 \xrightarrow{(7) \equiv (1)} A_2 \\ \text{MF 2: } A_2 &\xrightarrow{(2)} C_1 \xrightarrow{(5)} B_2 \xrightarrow{(6)} A_1 \end{aligned} \quad (16)$$

respectively. The step (7) is not explicitly shown in Fig. 4, since it is equivalent to (1). Applying Eq. 9, the parameters λ

and $\tilde{\lambda}$ simplify to

$$\lambda = -\tilde{\lambda} = \text{sgn}(\zeta_{A_1 A_2})\chi \quad (17)$$

where χ is the junction chirality.

Thus, using Eq. 17 and Eq. 9, we obtain the the result that the unitary time-evolution of the MFs γ_1 and γ_2 under exchange can be described by the unique braid-matrix

$$U = e^{\frac{\pi}{4}\chi\text{sgn}(\zeta_{12})\gamma_1\gamma_2} \quad (18)$$

where ζ_{12} is the tunneling amplitude of the segment separating γ_1 and γ_2 . The quantities ζ_{12} and χ for a specific network are calculated in the appendix.

VII. CONCLUSION

Non-Abelian statistics for MFs at the ends of TS nanowire segments can be realized by introducing time-varying gate-controllable tunnelings between MFs in a nanowire system to exchange the end MFs. Similar to the previous proposal for braiding MFs in 1D wires, our system can also be embedded in 3D leading to the possibility of non-Abelian statistics in 3D. The isolated MFs being exchanged in the tunneling geometry considered in this paper may be thought of as defects in a dimer lattice i.e. sites that are unpaired by tunneling. Alternatively, this system may also be thought of as a discretized implementation of the continuous nanowire network proposal of Alicea et. al.²⁶ However, the discrete implementation discussed in this paper allows us to compute the braid matrix explicitly in terms of MF overlaps. The non-Abelian braid matrix for exchange around a triangular loop geometry is given by a product of the fusion channel of the MFs $\zeta_{1,2}$ and the junction-chirality χ . The fusion channel $\zeta_{1,2}$ is simply the tunneling matrix-element between the MFs being exchanged and the junction-chirality is the product of tunneling terms around the triangular junctions. Thus the braid-matrix in the tunneling geometry considered in this paper is completely determined in terms of microscopic tunneling parameters by Eq. 18 making nanowire systems a well-controlled platform to realize non-Abelian statistics.

Acknowledgments

We thank Parsa Bonderson, Anton Akhmerov and Kirill Shtengel for helpful discussions. We are grateful to the Aspen Center for Physics for hospitality during the 2010 summer program *Low Dimensional Topological Systems*. D.J.C. is supported in part by the DARPA-QuEST program. S.T. acknowledges support from DARPA-MTO Grant No: FA 9550-10-1-0497. J.D.S. is supported by DARPA-QuEST, JQI-NSF-PFC, and LPS-NSA.

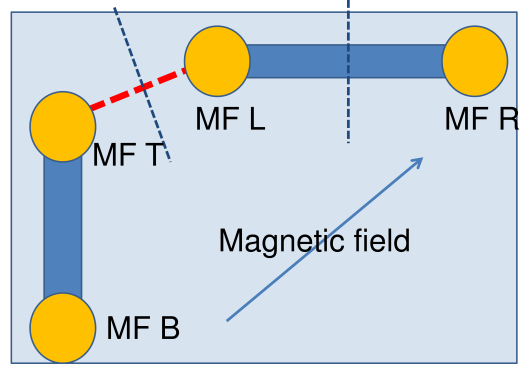


FIG. 5: (Color online) Schematic of orthogonal nanowire system on a superconductor (shown as light rectangle) that generates tunneling of MFs (shown as light orange discs). The entire system is subject to an in-plane magnetic field to generate Zeeman coupling. Nanowire segments in the TS phase are shown as dark blue rectangles with end MFs. Tunneling is generated between MF T and MF L by conventional tunneling across a nearly depleted nanowire in the NTS phase. The tunneling can be calculated using the Bardeen tunneling formula³³ as the matrix element of the current operator in the middle of the wire (black dotted line). Similarly tunneling is generated between MF L and MF B by lowering the topological gap so that the wave-functions have significant overlap at the middle of the wire (black dotted line).

Appendix A: Calculation of tunneling matrix elements for a specific nanowire system

In the main text of the paper we saw how controlling the tunneling between MFs can be used to generate transport of Majorana fermions from one point to another and eventually generate exchanges and braids that are useful for TQC. The sign of the resulting exchange was found to be determined by the signs of various tunneling matrix elements. While the existence of non-Abelian statistics is demonstrated in the paper in general, the signs of the tunneling matrix elements themselves are depend on the microscopic details of the system.

In this appendix, we calculate the tunneling matrix elements between the various MFs at a junction for a network of orthogonal wires on a superconducting substrate as shown in Fig. 5. A Zeeman potential is applied at 45 degrees to the wires. The wires in the TS phase (shown in dark blue), which support MFs (shown as orange discs) at their ends, are taken to have a Rashba spin-orbit coupling generated from interaction with the superconducting substrate. The Bogoliubov de Gennes (BdG) Hamiltonian for the wire along x is given by

$$H_{BdG} = (-\eta\partial_x^2 - \mu(x))\tau_z + V_z\sigma \cdot \hat{B} + i\alpha\partial_x\sigma_y\tau_z + \Delta\tau_x \quad (A1)$$

and for the wire along y is given by

$$H_{BdG} = (-\eta\partial_y^2 - \mu(y))\tau_z + V_z\sigma \cdot \hat{B} - i\alpha\partial_y\sigma_x\tau_z + \Delta\tau_x. \quad (A2)$$

The direction of the Zeeman field is $\hat{B} = (\hat{x} + \hat{y})/\sqrt{2}$. Following the spin-rotation and phase transformations in Ref. [20], for negative Rashba coupling $\alpha < 0$, the Majorana wave-functions at the left and the right ends of the x wires have

the form

$$\phi_L = \begin{pmatrix} u(x)e^{i\phi/2} \\ i\sigma_y u(x)e^{-i\phi/2} \end{pmatrix} \text{ and } \phi_R = i\sigma_x \begin{pmatrix} u(-x)e^{-i\phi/2} \\ i\sigma_y u(-x)e^{i\phi/2} \end{pmatrix} \quad (\text{A3})$$

respectively, where $\phi = \sin^{-1} \frac{V_Z}{\Delta\sqrt{2}}$ and $u(x)$ is a real 2-spinor. Note that in this geometry there is now an additional condition for the wire to be gapped i.e $\sqrt{\Delta^2 + \mu^2} < V_Z < \Delta\sqrt{2}$. This constraint implies $\frac{\pi}{4} < \phi < \frac{\pi}{2}$. The Majorana wave-functions for the Majorana fermions at the bottom and top ends of the wires parallel to the y axis have the form

$$\phi_B = Q \begin{pmatrix} u(y)e^{-i\phi/2} \\ i\sigma_y u(y)e^{i\phi/2} \end{pmatrix} \text{ and } \phi_T = iQ\sigma_x \begin{pmatrix} u(y)e^{i\phi/2} \\ i\sigma_y u(y)e^{-i\phi/2} \end{pmatrix} \quad (\text{A4})$$

respectively, where $Q = e^{-i\pi\sigma_z/4}$.

Transport of MFs is generated by introducing tunneling into the system of MFs shown in Fig. 5. The junction chirality χ defined in the paper depends only on the tunneling from 3 end MFs $\{L, R, T\}$ with wave-functions $\phi_{L,R,T}$. Let us start by considering the MF overlap across the NTS segments (shown as red dashed lines in Fig. 5) which is simplest to understand in the limit of low negative chemical potential $\mu = -|\mu|$ where $|\mu| \gg V_Z, \Delta$. Physically, this corresponds to a wire that is nearly depleted of electrons and only acts as a tunnel barrier. In such a case, the Majorana wave-function in the NTS wire has the usual exponentially decaying form $\Psi(x) = \Psi(x_I)e^{-\gamma|x-x_I|}$ as in a barrier, where $\gamma \sim \sqrt{2m|\mu|}$ and x_I is the position of the interface between the TS and NTS wire segments. The tunneling matrix elements ζ_{ij} between two MFs at $x_{I,1} = -a/2$ and $x_{I,2} = a/2$ across the NTS wire can be calculated from the matrix-elements of the current operator and the wave-functions in the middle of the wire³³ ($x = 0$ as shown by the dark dotted lines in Fig. 5)

$$\begin{aligned} \zeta &= \frac{1}{2}[\Psi_1^\dagger(0)\tau_z\partial_x\Psi_2(x)|_{x=0} - \partial_x\Psi_1^\dagger(x)|_{x=0}\tau_z\Psi_2(0)] \\ &- i\alpha\Psi_1^\dagger(0)\sigma_y\tau_z\Psi_2(0) \sim -\gamma e^{-\gamma a}\Psi_2^\dagger(-\frac{a}{2})\tau_z\Psi_1(\frac{a}{2}) \\ &= -\rho\Psi_2^\dagger(-\frac{a}{2})\tau_z\Psi_1(\frac{a}{2}) \end{aligned} \quad (\text{A5})$$

where $\rho = \gamma e^{-\gamma a}$ is the overall tunneling strength and we have assumed $\lambda \gg \alpha$. In this limit, the overlap between a pair of Majorana wave-functions $\Psi_1 = (u_1(x), i\sigma_y u_1^*(x))^T$ and $\Psi_2 = (u_2(x), i\sigma_y u_2^*(x))^T$ is given by $M = 2i\rho\text{Im}(u_1^\dagger u_2)$. This is purely imaginary and manifestly anti-symmetric as expected. Furthermore since the fundamental spinor $u(x)$ in terms of which each of $u_{1,2}$ are written is real, we can write

it as $u = (\cos\theta, \sin\theta)^T$, where the parameter θ depends on V_Z, μ, α etc. With the help of these relations it is easy to tabulate the Majorana tunneling matrix as an anti-symmetric matrix for the states in the order (L, R, T) as

$$\zeta = i\frac{\rho}{\sqrt{2}} \begin{pmatrix} 0 & \sqrt{2}\cos\phi\sin 2\theta & \sin 2\theta \\ * & 0 & (\sin\phi + \cos\phi\cos 2\theta) \\ * & * & 0 \end{pmatrix} \quad (\text{A6})$$

where the elements in the $*$ have been left empty since they are determined by the anti-symmetry constraint. The junction chirality χ in the previous section, used only the Majorana modes L, T, R and is calculated using the expression, $\chi = \zeta_{RL}\zeta_{LT}\zeta_{TR} = \rho^3\cos^2\phi\sin^2 2\theta[\cos 2\theta + \tan\phi]$, which is always positive, since $\tan\phi > 1$ for the Zeeman direction $\hat{B} = (\hat{x} + \hat{y})/\sqrt{2}$ and negative Rashba coupling $\alpha < 0$. Changing the Zeeman potential to $\hat{B} = (\hat{x} - \hat{y})/\sqrt{2}$ flips the chirality. Changing the sign of the Rashba coupling α requires us to change $\phi_L \rightarrow i(u(x)e^{i\phi/2}, -i\sigma_y u(x)e^{-i\phi/2})$. Since all the other wave-functions are derived from symmetry transformations applied to ϕ_L , the rest of the calculation goes through as is with the only difference that $u(x)$ changes to $iu(x)$. Therefore the final result for the chirality of the junction is independent of the Rashba coupling.

The signs acquired by MFs on exchange is dependent also on the tunneling between the MFs L, R across a TS segment. The tunneling amplitude between Majorana fermions on the same topological segment is well-controlled and can be calculated in the limit of a long topological wire (wire length $L > \alpha/V_Z$). In this limit, the MFs only overlap in the limit where the gate potential is tuned so that the wire is driven towards a phase transition by tuning μ near to $\mu = \sqrt{V_Z^2 - \Delta^2}$. The relevant slowest decaying spinor component then determines the tunneling matrix elements and is given by $u(x) = (V_Z + \text{sgn}(\alpha)\sqrt{V_Z^2 - \mu^2}, -\mu)^T \exp(-\frac{x}{|\alpha|}(\sqrt{V_Z^2 - \mu^2} - \Delta))$. The tunneling matrix element is given by $M \sim -i\alpha\Psi_L^\dagger\sigma_y\tau_z\Psi_R = -i\alpha\text{Re}[u_L^\dagger\sigma_y u_R]$. Substituting u , we find the overlap to simplify to $M \propto -i\alpha\cos\phi e^{-2L/\xi}$ where $\xi = |\alpha|/(\sqrt{V_Z^2 - \Delta^2} - \mu)$. Thus the sign of $\zeta_{L,R}$ is determined by the sign of the Rashba spin-orbit coupling α . Using these results together with Eq. A6, one can check the physically reasonable result that changing the sign of the Rashba coupling α , flips the sign of the MFs on interchange.

Thus, provided care is taken to ensure the conditions for the braid discussed in this section, the sign of both clock-wise exchanges is positive for positive Rashba coupling α and negative other-wise. For a given Rashba coupling the sign of the braid can be altered by considering anti-clockwise braids.

¹ A. Kitaev, Ann. Phys. **303**, 2 (2003).

² M. Freedman, A. Kitaev, M. Larsen, and Z. Wang, Bull. Am. Math. Soc. **40**, 31 (2003).

³ S. Das Sarma, M. Freedman, C. Nayak, Phys. Rev. Lett. **94**,

166802 (2005).

⁴ C. Nayak et al., Rev. Mod. Phys. **80**, 1083 (2008).

⁵ S. Bravyi and A. Kitaev, Annals of Physics, Vol. **298**, 210(2002).

⁶ S. Bravyi, A. Kitaev, Phys. Rev. A, **71**, 022316(2005).

- ⁷ F. Wilczek, Nature Physics **5**, 614 (2009); B. G. Levi, Physics Today **64**, 20(2011); A. Stern, Nature **464**, 187-193 (2011).
- ⁸ E. Majorana, Nuovo Cimento **5**, 171 (1937).
- ⁹ G. E. Volovik, The Universe in a Helium Droplet (Clarendon, Oxford, 2003).
- ¹⁰ N. B. Kopnin and M. M. Salomaa, Phys. Rev. B **44**, 9667 (1991).
- ¹¹ N. Read and D. Green, Phys. Rev. B **61** (2000) 10267.
- ¹² C. Zhang, V. W. Scarola, S. Tewari, S. Das Sarma, Proc. Natl. Acad. Sci. USA **104**, 18415 (2007).
- ¹³ L. Fu and C. L. Kane, Phys. Rev. Lett. **100**, 096407 (2008).
- ¹⁴ A. P. Schnyder, S. Ryu, A. Furusaki and A. W. W. Ludwig, Phys. Rev. B **78**, 195125 (2008).
- ¹⁵ A. Y. Kitaev, Physics-Uspekhi **44**, 131 (2001).
- ¹⁶ M. Sato, S. Fujimoto, Phys. Rev. B **79**, 094504 (2009).
- ¹⁷ J. D. Sau, R. M. Lutchyn, S. Tewari, and S. Das Sarma, Phys. Rev. Lett. **104**, 040502 (2010).
- ¹⁸ S. Tewari, J. D. Sau, S. Das Sarma, Ann. Phys. **325**, 219, (2010).
- ¹⁹ J. Alicea, Phys. Rev. B **81**, 125318 (2010).
- ²⁰ J. D. Sau et al. Phys. Rev. B **82**, 214509 (2010).
- ²¹ S. Tewari, J. D. Sau, S. Das Sarma, unpublished (2009).
- ²² R. M. Lutchyn, J. D. Sau and S. Das Sarma, Phys. Rev. Lett. **105**, 077001(2010); Y. Oreg, G. Refael, F. von Oppen, *ibid.* **105**, 17702 (2010).
- ²³ Y. J. Doh et al, Science **309**, 272 (2005).
- ²⁴ D. A. Ivanov, Phys. Rev. Lett. **86**, 268 (2001); A. Stern, F. von Oppen, and E. Mariani, Phys. Rev. B **70**, 205338(2004); N. Read, *ibid.* **79**, 045308(2009).
- ²⁵ M. Stone and S. Chung, Phys. Rev. B **73**, 014505(2006).
- ²⁶ J. Alicea et al. Nature Physics (2011).
- ²⁷ D. J. Clarke, J. D. Sau, S. Tewari, arxiv: 1012.0296 (2010).
- ²⁸ P. Bonderson, private communication.
- ²⁹ P. Bonderson, M. Freedman, C. Nayak, Phys. Rev. Lett. **101**, 010501 (2008).
- ³⁰ J. D. Sau, S. Tewari, S. Das Sarma, Phys. Rev. A **82**, 052322 (2010).
- ³¹ M. Cheng, R. M. Lutchyn, V. Galitski, S. Das Sarma, Phys. Rev. Lett. **103**, 107001 (2009); M. Cheng, R. M. Lutchyn, V. Galitski, S. Das Sarma, Phys. Rev. B **82**, 094504 (2010).
- ³² A. Y. Kitaev in a presentation at Aspen Workshop on *Low dimensional systems* (2010) argued that a similar result holds based on consevation of $i\gamma_1\gamma_2\gamma_3$ which follows from conservation of fermion parity.
- ³³ J. Bardeen, Phys. Rev. Lett. **6**, 57 (1961).